

Chemical sensing in the submillimeter wave regime

Samuel Mickan^{*a}, X.-C. Zhang^b Jesper Munch^c and Derek Abbott^{*a}

^aCentre for Biomedical Engineering (CBME) and Dept. of Electrical and Electronic Engineering,
Adelaide University, Australia

^bDepartment of Physics, Rensselaer Polytechnic Institute, NY, U.S.A.

^cDepartment of Physics, Adelaide University, Australia

ABSTRACT

T-ray systems offer an exciting range of capabilities for chemical and biological diagnostics using the emerging technology of terahertz pulse imaging.^{1,2} We report results from the first Australian T-ray program and discuss how MOEMS techniques can be applied to decrease the system size.³ A small portable T-Ray system will cost less and is needed, for example, in endoscopic applications.⁴

Key words: terahertz, MOEMS, biosensors.

1. INTRODUCTION

Pulsed T-ray chemical sensing has developed over the last fifteen years, exploring the previously inaccessible far-infrared region of the electromagnetic spectrum. New sources and detectors offer improved access to spectral information at terahertz (THz), or submillimeter, frequencies. Two new terahertz generation and detection techniques have been developed in the last ten years, both relying on ultra-fast laser pulses. The first, using photoconductive antennae, was developed at Bell Labs and IBM Watson Research Center and is now available in a commercial product from Picometrix Inc.⁵ The second, using the nonlinear effects of optical rectification and electro-optic sampling, has been developed at RPI and is now capable of showing two-dimensional images of terahertz radiation.⁶ Terahertz radiation has been used for an increasing range of chemical sensing applications, including biomedical diagnostics,⁷ semiconductor device diagnostics,⁸ trace gas analysis,⁹ moisture analysis for agriculture,¹⁰ quality control of packaged goods,¹¹ inspection of artwork and inspection of the internal structure of smart cards.¹²

Pulsed T-ray systems are well suited to complement existing chemical sensing and analysis tools, such as FTIR spectroscopy and NMR. Pulsed terahertz radiation consists of ultrashort pulsed radiation with a bandwidth spanning the range of about 0.1 to 10 THz. This corresponds to about 3 to 0.03 millimeters in wavelength, or about 3 to 300 cm⁻¹. A typical T-ray pulse is shown in Fig. 1. The vertical axis shows the magnitude of the pulse and the horizontal axis shows the time-delay between the optical generation and detection pulses. The T-ray pulse visible at about 20 ps is followed by oscillations caused by water vapour in the system.¹³ The operation of a T-ray system is explained in Sect. 3. The important characteristic of a T-ray pulse is its short pulse length. The picosecond pulse, that is 10⁻¹² seconds, has high peak power, short time resolution and a very broad spectral bandwidth. Pulsed T-ray detection is time gated, so achievable signal-to-noise ratios (SNRs) are far higher than non-gated techniques.¹⁴ Ultrafast laser-driven T-ray sources are brighter and more portable than other sources in this frequency range. Hot sources are very inefficient at such long wavelengths and water vapour lasers are cumbersome.¹⁵ Electronic sources have achieved frequencies only up the gigahertz range and are very low-powered.¹⁶ Although useful for terahertz space applications, these sources are not strong enough for spectroscopy or imaging. Pulsed T-ray systems have demonstrated SNRs of over 10,000:1 using lock-in detection,¹⁷ with only small pulse energies. A high powered pulse is 0.4 microjoules.¹⁸ Having very low average power, T-rays are particularly attractive for medical applications, when it is important to avoid damaging the sample. Characterised by high SNR and wide bandwidth, T-rays are an excellent tool for sensing and analyzing molecules and mixtures by their far-infrared spectra.

Current T-ray systems remain, however, limited in used because of their size, robustness and sensitivity. Although useful for analyzing gases, the power and sensitivity of a typical T-ray system is not sufficient to characterize thick samples. For example, femtojoule terahertz pulses of 0.3 – 2.7 THz are blocked by three millimeters of moist dermal tissue.¹⁹ This means many samples can only be characterised using a reflection geometry. In reflection, thick objects can be characterised by the far-infrared spectral response of their surfaces. Figure 7 shows the components

^{*}Email: spm@ieee.org, dabbott@eleceng.adelaide.edu.au

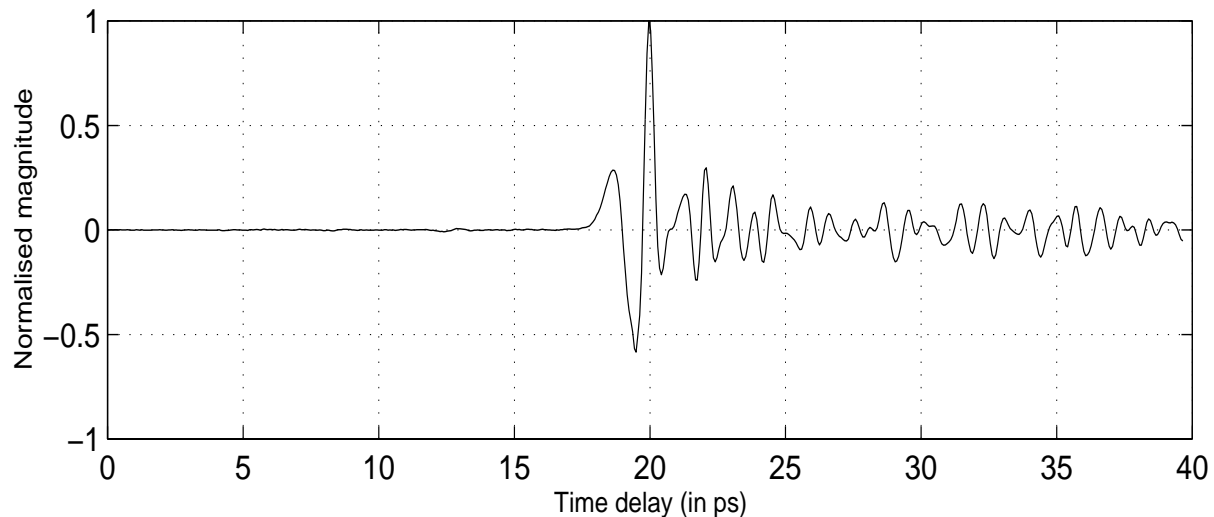


Figure 1. A terahertz pulse in free space. This was measured using an all-optical T-ray system driven by a 800 nm Ti:sapphire Hurricane (SP) laser running at 1 kHz repetition rate, with a pulse duration of 130 fs and optical power of 50 mW. The magnitude of this plot has been normalised to the peak value of the terahertz field in free-space transmission.

in a typical terahertz system designed for reflective measurements. The function of this system is further described in Sect. 3. Using a reflection geometry minimises the losses and distortions caused by terahertz radiation traveling through air by minimising the path length. Water in the atmosphere slightly reduces the amplitude of the terahertz radiation and imparts a ringing to the waveform.¹³ This can be seen in Fig. 1 as an oscillation on the tail of the pulse. The effects of water vapour can be removed by drying or evacuating the radiation path. This is quite difficult in a transmission geometry because the sample is part of the set-up. Using a reflection geometry, the path length can be minimised and the whole system can be combined in a sealed package. One final advantage of a reflection geometry in a pulse terahertz system is the potential for tomographic imaging, where a depth profile of the sample is built up by analyzing return pulses from internal structures in the sample.²⁰ Tomography is difficult in terms of calculations but requires no more hardware than discussed in the reflection system and can provide important information about a sample's subsurface structure.

We propose MOEMS for implementing a reflective T-ray system in a single compact package. This would improve stability, cost, portability and sensitivity. Excluding the ultra-fast pump laser, all the standard components of a terahertz system lend themselves to implementation in MOEMS. The components of the system are detailed in Sect. 3 below. Basically, the system requires two mirrors, two crystals for generation and detection, and a movable delay stage. A MOEMS terahertz system would be far easier to manufacture than large-scale systems, it could be easily sealed and evacuated, and the short path-length minimises unnecessary transmission losses. The following sections analyse the theoretical advantages of a minimum path-length terahertz system and discuss how it would be implemented. The conclusion presents some open problems with MOEMS implementation and other system improvements.

2. CHEMICAL SENSING

T-ray spectroscopy exposes the far-infrared or submillimeter region of the electromagnetic spectrum. The far-infrared is populated by energy transitions of less than 0.1 electron-volts, which corresponds to different rotational and torsional states of a whole molecule, as opposed to between atoms.²¹ For larger molecules, the far-infrared has fewer transitions than the near-infrared, which can be very densely populated. The far-infrared also corresponds to energy gaps in superconductors, plasma states, and lattice vibrations and other resonances in crystals.²² Typical terahertz waveforms are shown in Figs. 2 and 3. These pulses show characteristics of transmission through two crystals used extensively in T-ray experiments – zinc telluride and gallium arsenide. The spectra of these pulses are shown in Figs. 4

and 5. There are clear differences between the absorption spectra of the two crystals where lattice resonances are present; for example, the strong absorption band around 5 THz in the ZnTe sample. Pulsed terahertz spectroscopy is a coherent technique, where both the amplitude and phase of the terahertz pulse are measured. Coherent detection enables direct calculation of absorption and refraction profiles without using the Kramers-Kronig relations. T-ray spectroscopy has been used in a wide range of chemical sensing applications, including gas sensing,²³ nonpolar liquid spectroscopy,²⁴ semiconductor wafer characterisation²⁵ and time-resolved studies of liquid dynamics.²⁶

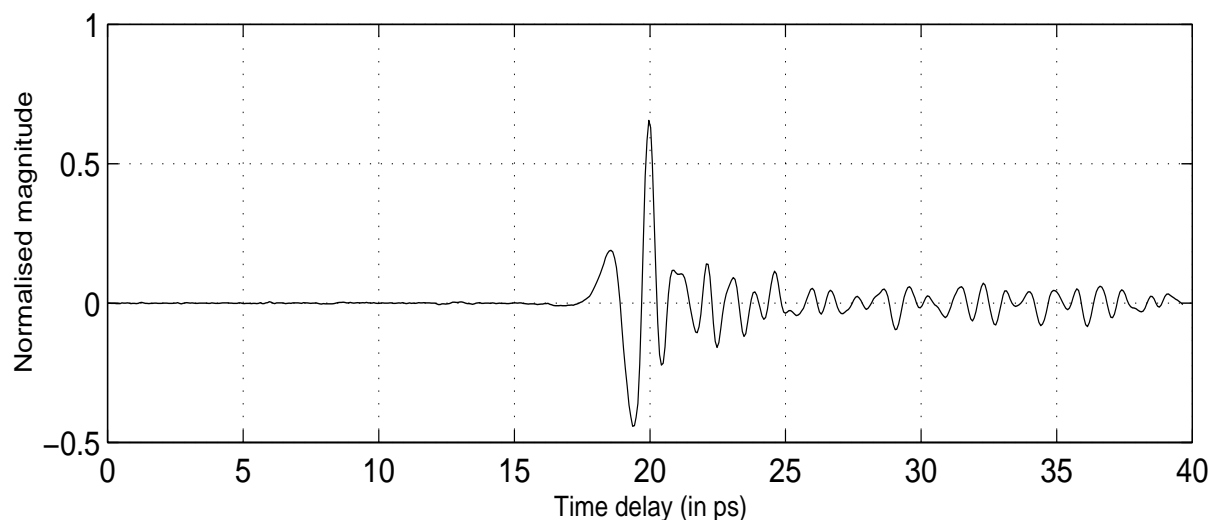


Figure 2. Terahertz pulse after passing through a 1mm-thick (110) ZnTe crystal. The Fourier transform of this waveform indicates the far-infrared absorption spectrum of the ZnTe, seen in Fig. 4. This pulse was obtained using a transmission geometry and a lock-in time constant of 100ms. The magnitude of this plot has been normalised to the peak value of the terahertz waveform in free space, shown in Fig. 1.

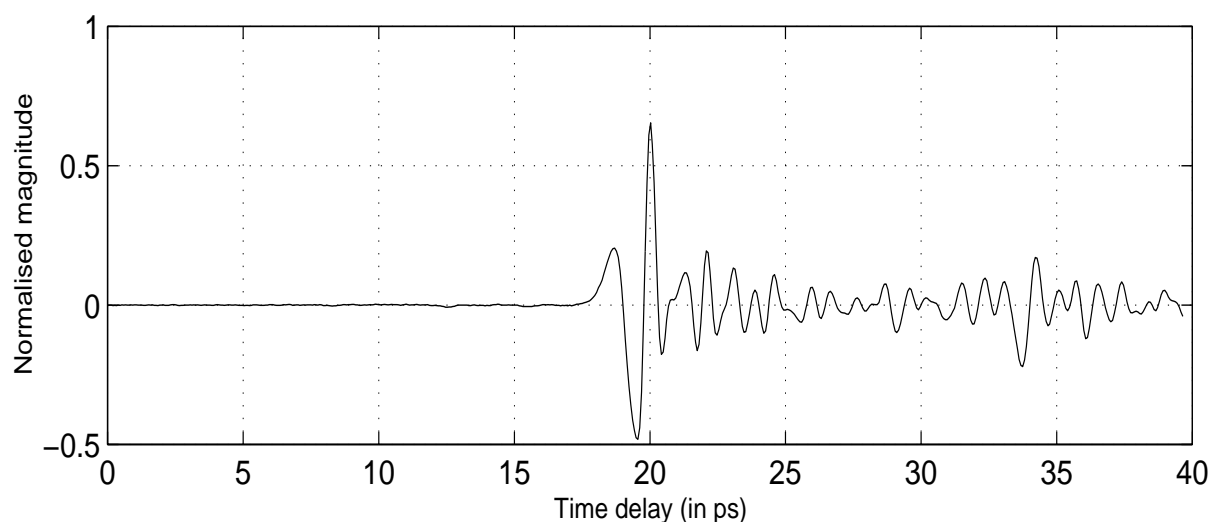


Figure 3. Terahertz pulse after passing through a 601 μ m-thick (110) SI-GaAs crystal. This pulse was obtained using a transmission geometry and a lock-in time constant of 100ms. The magnitude of this plot has been normalised to the peak value of the terahertz waveform in free space, shown in Fig. 1.

An important extension of T-ray spectroscopy is T-ray imaging, or terahertz pulse imaging (TPI). The first TPI

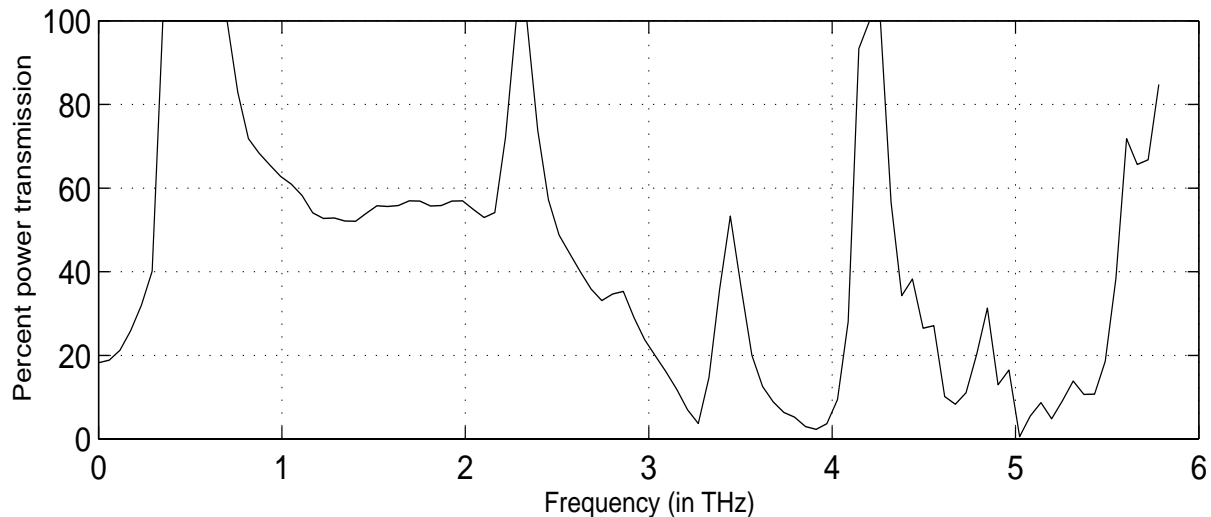


Figure 4. Absorption spectrum of a ZnTe crystal in the far-infrared. This spectrum is the ratio of the free-space terahertz power spectral density and the power spectral density of the terahertz pulse after transmission through a sample of 1mm-thick (110) ZnTe. The power spectral density was estimated by Welch's method. The x-axis has been limited to a maximum frequency of 6 THz because the power at higher frequencies is very small and the ratios are dominated by noise.

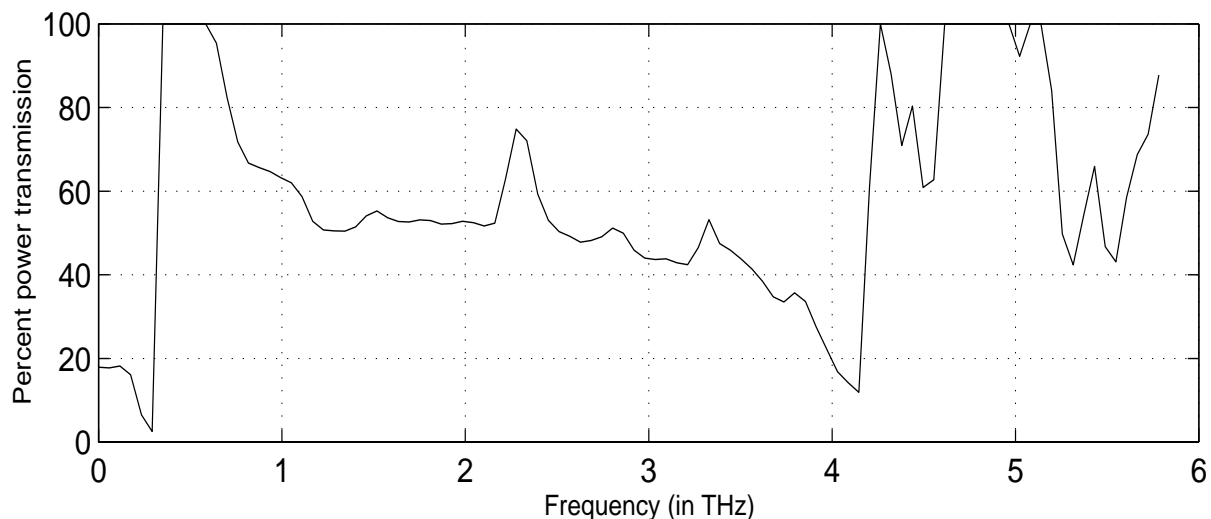


Figure 5. Absorption spectrum of a GaAs crystal in the far-infrared. This spectrum is the ratio of the free-space terahertz power spectral density and the power spectral density of the terahertz pulse after transmission through a sample of $601\mu\text{m}$ -thick (110) SI-GaAs.

systems involved raster scanning a sample to build up a two-dimensional image.²⁷ Recently, this has been extended to using a CCD camera to capture the terahertz image of the whole sample at once.^{28,29} Using a two-dimensional array of data speeds up the acquisition of information at the expense of losing signal power at each pixel. Simple contrast images in the terahertz domain can be developed, showing the cumulative absorption of a material in the terahertz bandwidth. Such an image is shown in Fig. 6. The three digits on the plastic \$100 note clearly have different absorption profiles in the far-infrared. This does not necessarily correspond to transmission at optical wavelengths. Dry substances, such as paper, transmit T-rays with less than 1% attenuation. More interesting than a

simple contrast image is a two-dimensional array of waveforms, such as those in Figs. 1, 2 and 3. Spectral analysis at each pixel can then provide molecular information about the whole sample. With a metric of far-infrared molecular classification, it will be possible to map samples in terms of their specific chemistry. T-ray chemical sensing and imaging will become a valuable tool in medical and biological diagnostics.

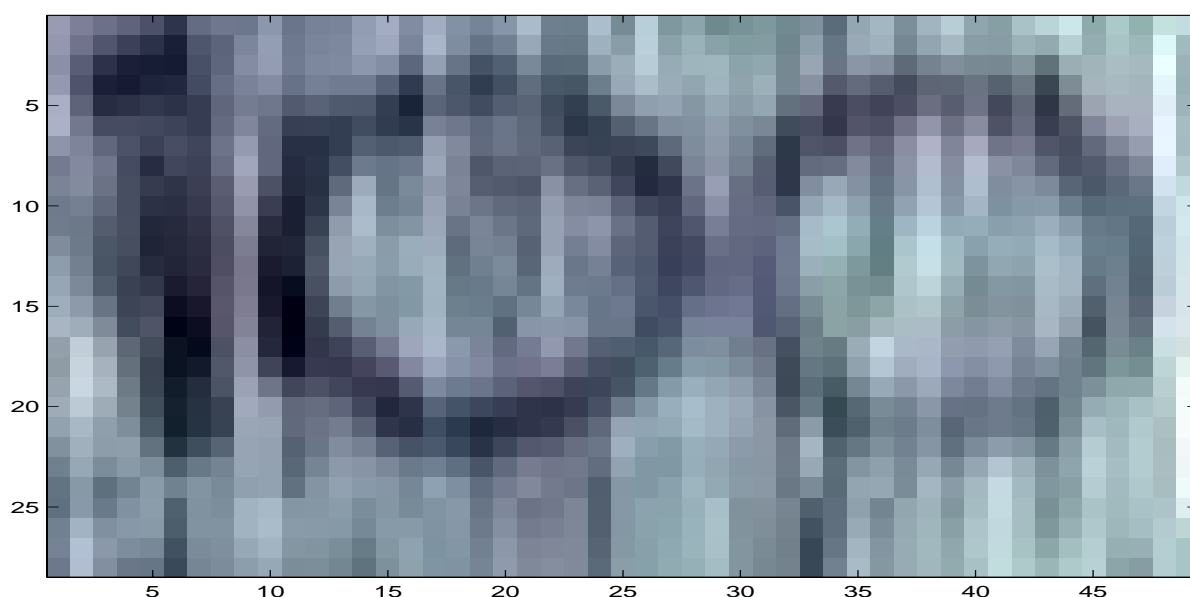


Figure 6. Two-dimensional terahertz image plotting difference in terahertz absorption profile of a segment of a plastic Australian \$100 note. The dark pixels are points of higher absorption and the lighter pixels show greater transmission. The colour of each data point corresponds to the magnitude of peak of the terahertz pulse - darker pixels correspond to a smaller peak on the pulse. The image was built up by raster scanning the \$100 note through the terahertz beam in a transmission geometry.

T-ray chemical sensing has in recent years been applied to a number of biological problems. As mentioned above, T-rays are strongly attenuated by moist tissue because of water absorption. This has limited medical applications to dry or thin samples. Toshiba, for example, have explored T-ray images of human teeth.¹⁹ The T-ray data revealed differences between the enamel, the enamel and dentine and a cavity. T-ray images of living plant leaves and thin samples of wood have been studied to show water and density profiles.³⁰ Rice University has shown terahertz profiles of burnt chicken tissue² and we have studied thin slices of Spanish ham ('Jamon Serrano').³¹ The problems with biological imaging are resolution, penetration and speed. The resolution is limited by wavelength in the far field, giving about 0.3 mm resolution at 1 Terahertz, which will be sufficient for many biological applications. Depth penetration is a greater problem, even for reflection spectroscopy. Depth penetration can be improved by increasing the terahertz power and reducing the path length. Lastly, the imaging speed is important for living samples that tend to move. Therefore the CCD two-dimensional imaging technique can be used to minimise motion between the emitter and the sample. A MOEMS T-ray imaging system would help solve these problems.

3. MOEMS SYSTEM

Pulsed T-ray systems are based on an ultrafast laser set up in a pump-probe configuration.¹⁴ Figure 7 shows the main components of a reflective T-ray system.^{28,32} The ultrafast laser outputs femtosecond light pulses onto the terahertz emitter, generating T-rays, which are focussed onto the sample. Reflected radiation from the sample passes through a detector collinearly with a fraction of the femtosecond pulse. In a system with photoconductive antennae, the detector converts the terahertz pulse directly into an electric current. In electro-optic detection, the terahertz modulates the polarisation of the collinear femtosecond pulse in the detector crystal. The polarisation modulation is in turn converted to an intensity modulation using crossed polarisers. The output intensity modulation can be detected by a photodiode or cast onto a CCD camera. The delay stage changes the time difference between the

optical pulses incident on the emitter and detector. This time delay corresponds to the horizontal axes of Figs. 1, 2 and 3. Because the time delay must be zero within the travel of the delay stage, annotation (a) in the diagram indicates a longer path to balance the path length in both arms. The sample is placed to reflect T-ray onto the detector from its surface. The Fourier spectrum of reflected T-rays can be calculated from the reflected pulse. To determine the absorption spectrum of the sample, the spectrum of an unmodulated T-ray pulse must be measured by replacing the sample with a mirror. The sample's absorption spectrum is then the ratio of the spectra from the mirror and the sample itself. In measuring the reflected pulse, it is important to ensure the sample surface and the mirror are placed at exactly the same distance from the generation and detection setup. If the pulses travel different distances for the two cases, there will be phase errors in the analysis.

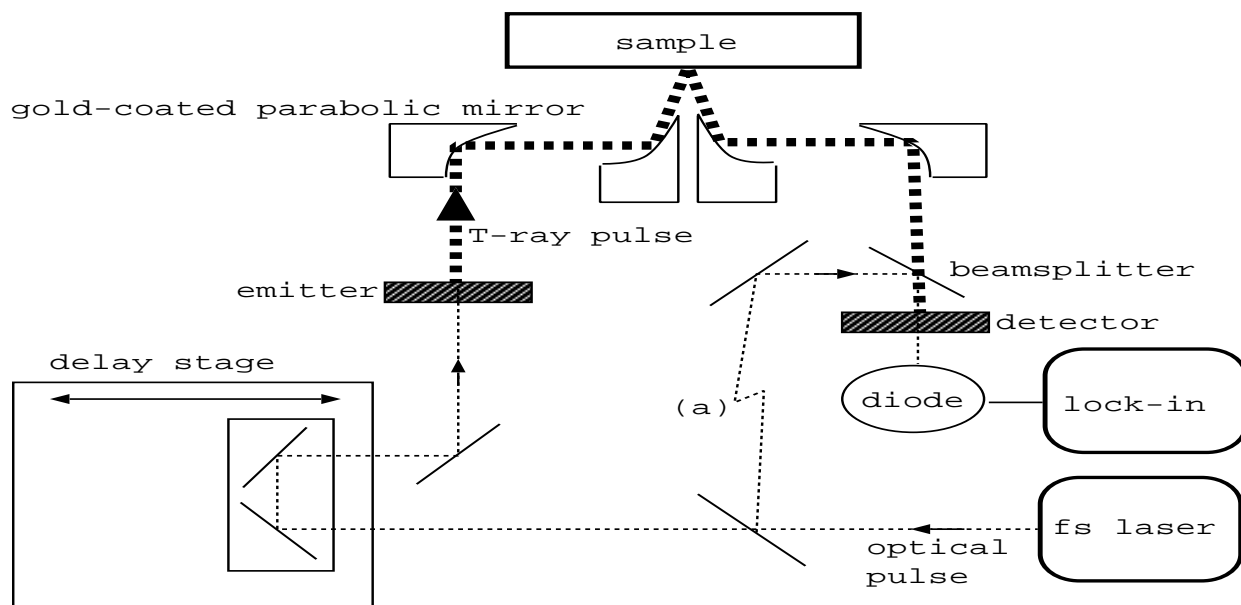


Figure 7. Outline of a typical reflective terahertz system. The laser generates ultrafast optical pulses, typically of femtosecond duration at about 800 nm. Each pulse is divided in a 0.95:0.05 ratio as the pump and probe respectively. The pump passes through a delay stage and into the emitter, whence T-rays are produced. The T-rays are collimated and focussed using gold-plated parabolic mirrors. Some terahertz radiation is reflected by the sample and focussed onto a detector. The detector modulates the probe pulse depending on the strength of the terahertz and a diode detects the intensity of the modulated probe pulse. Annotation (a) indicates an extended path length for the probe pulse, simplified here for clarity. The path length from the laser to the detector must be the same for both pump and probe pulses so that pulses are coincident within the travel of the delay stage.

We propose a number of improvements on the common T-ray setup by unifying the system into one package. A single sealed short path-length unit will be more robust, less expensive, easier to deploy and more sensitive than the configuration described above. Our proposed short path-length setup is outlined Fig. 8. The essential elements of a pulsed T-ray system are contained in the double lined box. The ultrafast laser remains external to the system and the femtosecond pulse enters through a small window. The small mirror in the centre of the unit splits the incoming pulse in an approximate 0.95/0.05 ratio corresponding to pump and probe pulses. The pump pulse falls on the zinc telluride emitter, generating terahertz radiation, which passes through a filter and is immediately reflected from the sample. The RG-1000 Schott colour glass filter blocks the remaining optical pulse. The probe pulse from the centre passes through a quarter wave plate and is reflected from a mirror onto the detector zinc telluride crystal. The quarter wave plate rotates the polarisation of the probe pulse so it is not reflected by the central mirror. Terahertz radiation from the sample is reflected by the larger mirror onto the detector crystal and travels collinearly with the probe pulse, rotating its polarisation. The probe pulse exits the unit and is detected by a photodiode or a CCD camera for images. In effect, the short path-length system operates identically to the system in Fig. 7.

A unique characteristic of this system is the positioning of the emitter crystal in the return path of the reflected

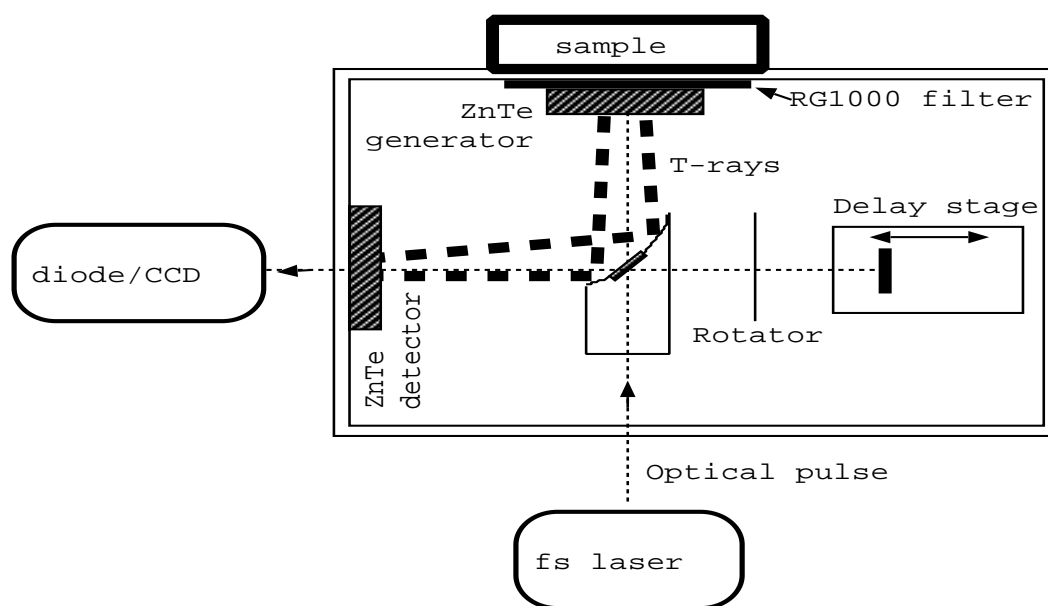


Figure 8. Design of a short path-length reflective terahertz system. The optical pulse from the laser enters the box and is divided into pump and probe pulses. The pump pulse excites the emitter. T-rays are reflected from the sample back through the emitter and are focussed onto the detector. The probe pulse is delayed and directed to the detector, where it is modulated by the terahertz radiation. The intensity of the modulated probe pulse is measured with a photodiode or CCD camera. The path length of the terahertz radiation has been minimised and the entire system is contained in a single box.

terahertz beam. We have profiled the terahertz absorption spectra of two common emitters, ZnTe and SI-GaAs, to measure their attenuation of the T-ray pulses. From the graphs in Figs. 4 and 5 above, SI-GaAs is seen to have a smaller absorption profile, which makes it a more desirable emitter for our configuration. Furthermore, at frequencies higher than those measured in Fig. 5, GaAs has better absorption characteristics: ZnTe absorbs strongly at its transverse-optical (TO) phonon frequency of 5.31 THz, whereas GaAs has a TO phonon at 8.06 THz.³³ The ZnTe absorption band around 5 THz is visible in Fig. 4, where GaAs has above 50% transmission. For experiments stretching to higher frequencies,³⁴ which provide better imaging resolution, GaAs will transmit more terahertz radiation than ZnTe.

The differences between a short path-length system and a normal system are having the contents in a single unit, enclosing the terahertz radiation in an airless case and the close proximity between the emitter and the sample. The unit can be evacuated and kept completely clean inside, reducing losses and improving stability once aligned. Having the sample in contact with the emitter removes losses from terahertz transmission in air and means the detection can be calibrated to a set terahertz path length. The sample window can easily be kept motionless relative to the sample, which is important for living samples. Having a sealed container is also an advantage when working in unclean medical or industrial environments. The short path-length T-ray system is ideally suited to a partial MOEMS implementation. The only moving part is the delay stage, which could be realised with a MEMS component. The crystals and mirror could be miniaturised and combined into a unit no more than a few centimeters in size. Such a unit would be a valuable step towards creating an endoscopic T-ray spectroscopic imaging system. The short-path implementation has advantages both for construction and application.

4. CONCLUSION

In conclusion, we have described a novel T-ray spectroscopic imaging system, designed for a short path-length, small size and robustness. Further improvements would come from reducing the size and cost of the ultrafast pump laser, currently the most cumbersome item in any terahertz system. Ultrafast fibre lasers are now an alternative to the larger and more expensive Ti:sapphire mode-locked lasers.³⁵ A fibre pump laser would enable full fibre coupling,

useful for an endoscopic implementation. The single mechanical element in the short path-length system, the delay stage, could be removed if a spatial transform method were used to detect the terahertz pulse. One technique is to directly measure the terahertz spectrum with a chirped optical pulse and a grating.³⁶ Another is to observe the terahertz time domain pulse shape by directing the probe pulse into the detection crystal on an angle and detecting the intensity with a linear diode array.^{37,38} To improve the penetration depth into the sample, signal-to-noise ratio and speed of the system, future research will address the emission and detection crystals and improve signal processing methods.^{39,40}

The open questions facing a short path-length T-ray spectroscopic system centre around (1) the techniques for MOEMS implementation, (2) speeding up signal acquisition and (3) characterising important molecules and mixtures in the far-infrared.

ACKNOWLEDGMENTS

This work was funded by the Australian Research Council (ARC). Thanks are due to Prof. X-C Zhang's group at Rensselaer Polytechnic Institute (RPI) for their assistance with the measurements.

REFERENCES

1. D. Arnone, C. Ciesla, and M. Pepper, "Terahertz imaging comes into view," *Physics World* (4), pp. 35–40, 2000.
2. D. M. Mittleman, M. Gupta, R. Neelamani, R. G. Baraniuk, J. V. Rudd, and M. Koch, "Recent advances in terahertz imaging," *Applied Physics B: Lasers and Optics* **68**(6), pp. 1085–1094, 1999.
3. S. Mickan, D. Abbott, J. Munch, X. C. Zhang, and T. van Doorn, "Analysis of system trade-offs for terahertz imaging," *Microelectronics Journal* **31**, pp. 503–514, 2000.
4. M. Li, X.-C. Zhang, G. D. Sucha, and D. J. Harter, "Portable terahertz system and its applications," in *Proceedings of SPIE*, vol. 3616, pp. 126–135, 1999.
5. D. Zimdars and J. V. Rudd, "Opening the terahertz window," *Photonics Spectra*, pp. 146–149, 2000.
6. Q. Chen and X.-C. Zhang, "Polarization modulation in optoelectronic generation and detection of terahertz beams," *Applied Physics Letters* **74**(23), pp. 3435–3437, 1999.
7. P. Y. Han, G. C. Cho, and X.-C. Zhang, "Time-domain transillumination of biological tissues with terahertz pulses," *Optics Letters* **25**(4), pp. 242–244, 2000.
8. W. J. Walecki, D. Some, V. G. Kozlov, and A. V. Nurmikko, "Terahertz electromagnetic transients as probes of a two-dimensional electron gas," *Applied Physics Letters* **63**(13), pp. 1809–1811, 1993.
9. R. H. Jacobsen, D. M. Mittleman, and M. C. Nuss, "Chemical recognition of gases and gas mixtures with terahertz waves," *Optics Letters* **21**(24), pp. 2011–2013, 1996.
10. S. Hadjiloucas, L. S. Haratzas, and J. W. Bowen, "Measurements of leaf water content using terahertz radiation," *IEEE Transactions on Microwave Theory and Techniques* **47**(2), pp. 142–149, 1999.
11. M. May, "T-rays spell sharper, safer images," *New Scientist* **154**(2083), p. 22, 1997.
12. M. C. Nuss, "Chemistry is right for T-rays," *IEEE Circuits and Devices* **12**(2), pp. 25–30, 1996.
13. M. van Exter, C. Fattinger, and D. Grischkowsky, "Terahertz time-domain spectroscopy of water vapour," *Optics Letters* **14**(20), pp. 1128–1130, 1989.
14. J. A. Valdmanis, G. Mourou, and C. W. Gabel, "Picosecond electro-optic sampling system," *Applied Physics Letters* **41**(3), pp. 211–212, 1982.
15. B. Lax, "Applications of far infrared lasers," in *Tunable Lasers and Applications*, A. Mooradian, T. Jaeger, and P. Stokseth, eds., vol. 3 of *Springer Series in Optical Sciences*, pp. 340–347, Springer-Verlag, Berlin, 1976.
16. H. Eisele, A. Rydberg, and G. I. Haddad, "Recent advances in the performance of InP Gunn devices and GaAs TUNNETT diodes for the 100–300-GHz frequency range and above," *IEEE Transactions on Microwave Theory and Techniques* **48**(4), pp. 626–631, 2000.
17. M. van Exter and D. Grischkowsky, "Characterization of an optoelectronic terahertz beam system," *IEEE Transactions on Microwave Theory and Techniques* **38**(11), pp. 1684–1691, 1990.
18. E. Budiarto, J. Margolies, S. Jeong, J. Son, and J. Bokor, "High-intensity terahertz pulses at 1-kHz repetition rate," *IEEE Journal of Quantum Electronics* **32**(10), pp. 1839–1846, 1996.

19. D. D. Arnone, C. M. Ciesla, A. Corchia, S. Egusa, M. Pepper, J. M. Chamberlain, C. Bezant, E. H. Linfield, R. Clothier, and N. Khammo, "Applications of terahertz (THz) technology to medical imaging," in *Proceedings of SPIE - Conference on Terahertz Spectroscopy and Applications*, vol. 3828, pp. 209–219, SPIE, (Munich, Germany), 1999.
20. D. M. Mittleman, S. Hunsche, L. Boivin, and M. C. Nuss, "T-ray tomography," *Optics Letters* **22**(12), pp. 904–906, 1997.
21. G. W. Chantry, *Submillimeter Spectroscopy*, Academic Press, New York, 1971.
22. J. T. Houghton and S. D. Smith, *Infra-red Physics*, Oxford University Press, Oxford, 1966.
23. D. M. Mittleman, R. H. Jacobsen, R. Neelamani, R. G. Baraniuk, and M. C. Nuss, "Gas sensing using terahertz time-domain spectroscopy," *Applied Physics B: Lasers and Optics* **67**(3), pp. 379–390, 1998.
24. J. E. Pedersen and S. R. Keiding, "THz time-domain spectroscopy of nonpolar liquids," *IEEE Journal of Quantum Electronics* **28**(10), pp. 2518–2522, 1992.
25. D. M. Mittleman, J. Cunningham, M. C. Nuss, and M. Geva, "Noncontact semiconductor wafer characterization with the terahertz Hall effect," *Applied Physics Letters* **71**(1), pp. 16–18, 1997.
26. D. S. Venables and C. A. Schmuttenmaer, "Time-resolved THz studies of liquid dynamics," in *Ultrafast Phenomena XI*, T. Elsaesser, J. G. Fujimoto, D. A. Wiersma, and W. Zinth, eds., vol. 63 of *Springer Series in Chemical Physics*, pp. 565–567, Springer-Verlag, Berlin, 1998.
27. B. B. Hu and M. C. Nuss, "Imaging with terahertz waves," *Optics Letters* **20**(16), pp. 1716–1718, 1995.
28. D. M. Mittleman, R. H. Jacobson, and M. C. Nuss, "T-ray imaging," *IEEE Journal of Selected Topics in Quantum Electronics* **2**(3), pp. 679–692, 1996.
29. X.-C. Zhang, "Ultrafast electro-optic field sensor and its image applications," in *OSA TOPS on Ultrafast Electronics and Optoelectronics*, M. Nuss and J. Bowers, eds., vol. 13, OSA, 1997.
30. M. Koch, "THz imaging: Fundamentals and biological applications," in *Proceedings of SPIE - Conference on Terahertz Spectroscopy and Applications*, vol. 3828, pp. 202–208, SPIE, (Munich, Germany), 1999.
31. B. Ferguson and D. Abbott, "Signal processing for t-ray bio-sensor systems," in *Proceedings of SPIE's 2000 Symposium on Smart Materials and MEMS*, SPIE, (Melbourne, Australia), 2000.
32. Q. Wu and X.-C. Zhang, "Design and characterization of travelling-wave electrooptic terahertz sensors," *IEEE Journal of Selected Topics in Quantum Electronics* **2**(3), pp. 693–700, 1996.
33. Q. Wu, M. Litz, and X.-C. Zhang, "Broadband detection capability of ZnTe electro-optic field detectors," *Applied Physics Letters* **68**(21), pp. 2924–2926, 1996.
34. Q. Wu and X.-C. Zhang, "Free-space electro-optic sampling of mid-infrared pulses," *Applied Physics Letters* **71**(10), pp. 1285–1286, 1997.
35. M. Li, G. Sucha, P.-Y. Han, A. Galvanauskas, D. Harter, and X.-C. Zhang, "THz generation and detection using 1550-nm pulses from a fiber laser," in *Conference on Lasers and Electro-Optics '00*, IEEE LEOS & OSA, (San Francisco, CA, U.S.A.), 2000.
36. Z. Jiang and X.-C. Zhang, "Single-shot spatiotemporal terahertz field imaging," *Optics Letters* **23**(14), pp. 1114–1116, 1998.
37. A. S. Weling, M. Bonn, J. Shan, G. A. Reider, A. Nahata, and T. F. Heinz, "Simultaneous recording of THz waveforms by multi-channel electro-optic detection," in *Ultrafast Electronics and Optoelectronics*, vol. 28 of *OSA TOPS*, pp. 95–97, OSA, (Snowmass, Col. U.S.A.), 1999.
38. J. Shan, A. S. Weling, E. Knoese, L. Bartels, M. Bonn, A. Nahata, G. A. Reider, and T. F. Heinz, "Single-shot measurement of terahertz electromagnetic pulses by use of electro-optic sampling," *Optics Letters* **25**(6), pp. 426–428, 2000.
39. P. Y. Han, M. Tani, F. Pan, and X.-C. Zhang, "Use of the organic crystal DAST for terahertz beam applications," *Optics Letters* **75**(9), pp. 675–677i, 2000.
40. L. Duvillaret, F. Garet, and J.-L. Coutaz, "Highly precise determination of optical constants and sample thickness in terahertz time-domain spectroscopy," *Applied Optics* **38**(2), pp. 409–415, 1999.